International Journal of Minerals, Metallurgy and Materials
Volume 18, Number 4, August 2011, Page 407
DOI: 10.1007/s12613-011-0454-5

High-temperature properties and microstructure of Mo microalloyed ultra-high-strength steel

Qi-hang Han[1)], *Yong-lin Kang*[1,2)], *Xian-meng Zhao*[1)], *Lu-feng Gao*[1)], *and Xue-song Qiu*[1)]

1) School of Materials Science and Engineering, University of Science and Technology Beijing, Beijing 100083, China

2) State Key Laboratory for Advanced Metals and Materials, University of Science and Technology Beijing, Beijing 100083, China

(Received: 26 July 2010; revised: 3 September 2010; accepted: 20 September 2010)

Abstract: The high-temperature mechanical properties and microstructure of forging billets of C-Si-Mn-Cr and C-Si-Mn-Cr-Mo ultra-high-strength cold-rolled steels (tensile strength≥1000 MPa, elongation≥10%) were studied. Through the comparison of reduction in area and hot deformation resistance at 600-1300°C, the Mo-containing steel was found to possess a higher strength and a better plasticity than the Mo-free one. The equilibrium phase diagram and atom fraction of Mo in different phases at different temperatures were calculated by Thermo-Calc software (TCW). The results analyzed by using transmission electron microscopy and TCW show that precipitates in the Mo-containing steel are primarily $M_{23}C_6$, which promote pearlite formation. The experimental data also show that a lower ductility point existing in the Mo-free steel at 850°C is eliminated in the Mo-containing one. This is mainly due to the segregation of Mo at grain boundaries investigated by electron probe microanalysis (EPMA), which improves the strength of grain boundaries.

Keywords: high strength steels; high temperature properties; microstructure; molybdenum; thermodynamics

[*This work was financially supported by the National High-tech Research and Development Program of China (No.2009AA03Z518).*]

1. Introduction

The automotive industry is constantly aiming to reduce weight, increase performance and safety, and rationalize production methods. The use of high-strength steels with good formability and weldability is increasingly considered as one important way in which these aims can be met. The attention of present research activities is devoted to advanced high-strength steel (AHSS) and ultra-high-strength steel (UHSS) [1-2].

Loss of ductility at high temperature is a problem occurring during the straightening operation of the continuous casting of steel. This is attributed to a tensile strain of 1%-2% at a strain rate between 10^{-3} and 10^{-4} s^{-1} generating on the top surface of a slab/billet [3-7]. Nb precipitates as niobium carbonitride (NbCN) at austenite grain boundaries preventing dynamic recrystallization and giving rise to low ductility intergranular failure [8]. B segregation and its effect on austenitic grain boundaries play an important role in the enhancement of hot ductility during high-temperature deformation and dynamic recrystallization [6, 9-11]. V acts in a similar manner to Nb but has a reduced effect because of high solubility of vanadium nitride (VN) in austenite [12-13].

Hot deformation resistance is very sensitive to microstructural change in high-temperature range. In order to make proper control of microstructure, the relation between microstructural change and deformation resistance must be obtained. Further, it is necessary to make clear the effect of microstructure on the hot deformation resistance to predict roll force in controlled rolling process with good accuracy [14-15].

Both of the steels are applied to automotive parts, such as bumpers and seat frames to meet the demands of weight re-

Corresponding author: Yong-lin Kang E-mail: kangylin@ustb.edu.cn

duction [16]. The aim of this paper is to study the effect of Mo on the high-temperature microstructure and properties by direct hot rolling of ultra high-strength cold-rolled steels.

2. Experimental

The chemical composition of the steels is listed in Table 1. The tensile strength and elongation of both the steels after cold rolling and annealing are more than 1000 MPa and 10%, respectively, with the thickness of strips from 1.2 to 1.8 mm.

Table 1. Chemical composition of the studied steels wt%

Steel	C	Si	Mn	Cr	Mo
Mo-free steel	≤0.19	≤0.7	≤2.2	≤0.6	—
Mo-containing steel	≤0.19	≤0.7	≤2.2	≤0.6	≤0.3

The samples were machined from a forging billet before hot rolling. The dilatometric behavior of experimental steels was observed during heating procedures using an ADAMEL DT1000 quenching dilatometer. An Gleeble 1500 simulator was used for the evaluation of hot ductility and hot strength.

For hot ductility experiment, the specimens were heated to 1300°C first and held for 180 s to homogenize the microstructure and to obtain a similar initial grain size. Then, the specimens were cooled down to the test temperatures (600-1300°C), held again for 30 s, and strained until failure at a constant true strain rate of 4×10^{-3} s^{-1}. Immediately after rupture, the broken specimens were quenched. Hot ductility was quantified by reduction in area at fracture. The fracture profiles were examined by JEM-2000FX transmission electron microscope and JEOL JXA-8100 electron probe microanalysis.

For hot deformation experiment, the specimens were heated to 1200°C and held for 180 s. Then, they were cooled to 1100-800°C and soaked for 10 s prior to deformation. The strain rates of 0.1 and 1 s^{-1} were chosen with the strain accumulated value of 60% at each deformation temperature.

3. Results

Fig. 1 shows the dilatometric behavior of the both steels during heating. There are two clear flexion points in both the alloys. The transformation temperatures A_{c1} (start of ferrite to austenite transformation) and A_{c3} (end of ferrite to austenite transformation) are 728 and 861°C for the Mo-free steel, and 731 and 855°C for the Mo-containing one, respectively. [0] This means that Mo would not affect the high-temperature properties by changing the transformation points.

The plots of reduction in area against test temperatures for both the steels examined in the present work are shown in Fig. 2. It is clear that experimental steels show two or three ductility troughs; however, the depth and the width of the trough vary with steel composition. The Mo-containing steel shows a better ductility. It is also investigated that the poorer ductility point existing in the Mo-free steel at 850°C is eliminated in the other one.

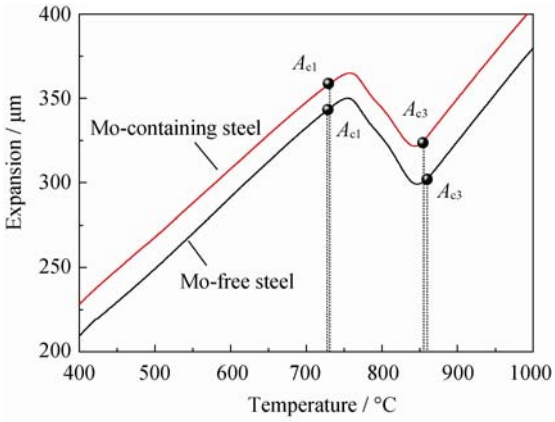

Fig. 1. Dilatometric behavior of experimental steels observed on heating procedures.

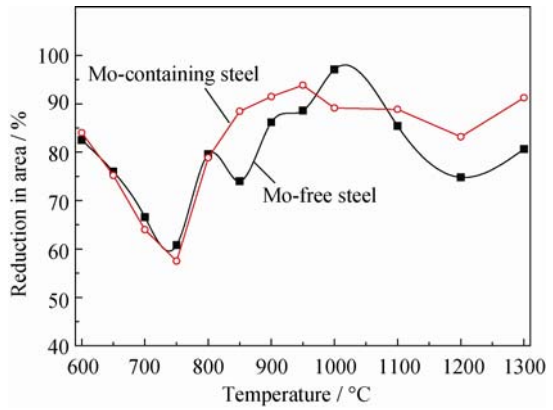

Fig. 2. Hot ductility curves for experimental steels.

Fig. 3 shows that the true stresses ($\sigma_{0.4}$) at different temperatures when the true strain is 40%. The $\sigma_{0.4}$ of Mo-containing steel is higher than that of Mo-free one, and it decreases quickly than Mo-free one with increasing deformation temperature. It is found that the critical temperature is 1100°C at the strain rate of 0.1 s^{-1}, and this temperature will decrease to 1000°C with increasing the strain rate to 1 s^{-1}.

The Thermo-Calc software is used to obtain the relationship between temperature and equilibrium phases for both the compositions, and the results is shown in Fig. 4. By the Thermo-Calc software calculation, both steels have M_7C_3 precipitations at 626°C. Besides, there are $M_{23}C_6$ precipita-

tions in the Mo-containing steel at 716°C, and they dissolved completely under 618°C.

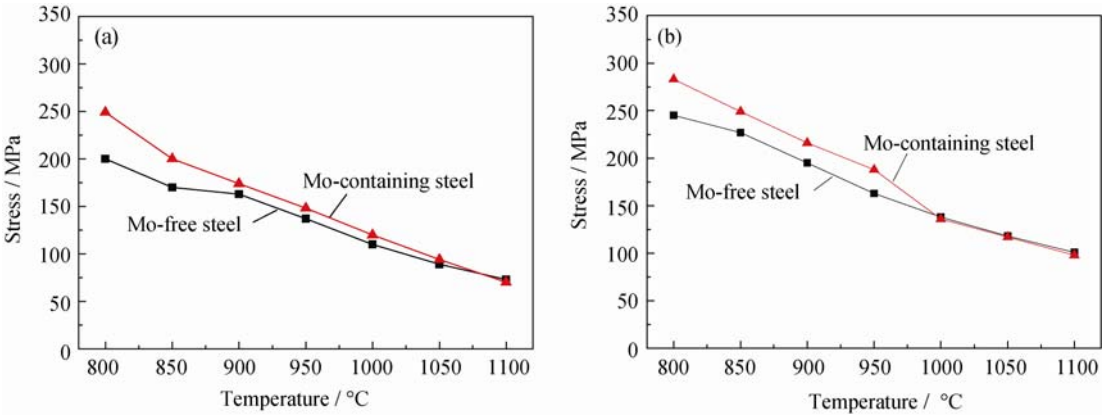

Fig. 3. True stresses of both the steels at different temperatures under the strain of 40% at different strain rates: (a) 0.1 s^{-1}; (b) 1 s^{-1}.

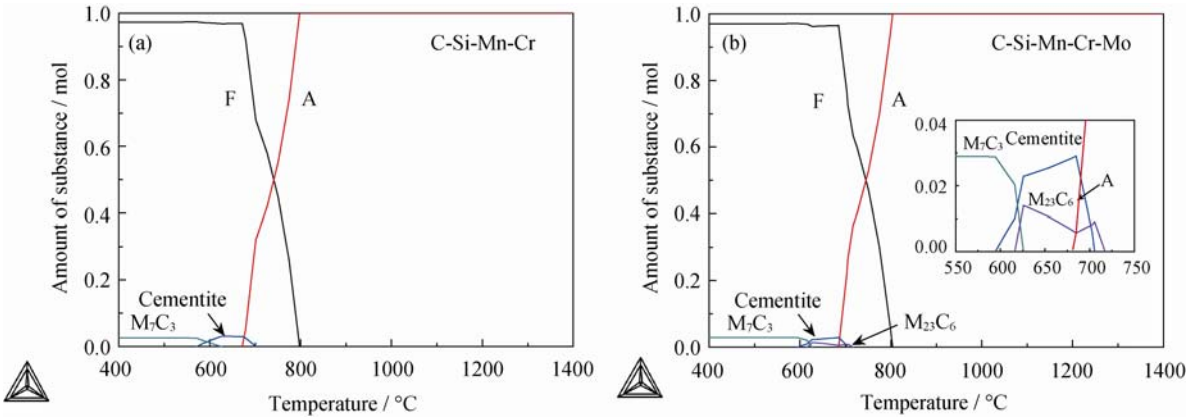

Fig. 4. Relationship between temperature and equilibrium phases calculated by Thermo-Calc at 1000 K and 101325 Pa with the system size of 1 mol: (a) C-Si-Mn-Cr; (b) C-Si-Mn-Cr-Mo.

The plot of temperature versus the amount of all phases containing in $M_{23}C_6$ is shown in Fig. 5. The $M_{23}C_6$ is composed of Fe, C, Cr, Mn, and Mo. The amount of Cr is higher than Mo in $M_{23}C_6$; however, this phenomenon will be inverse in M_7C_3 by calculation.

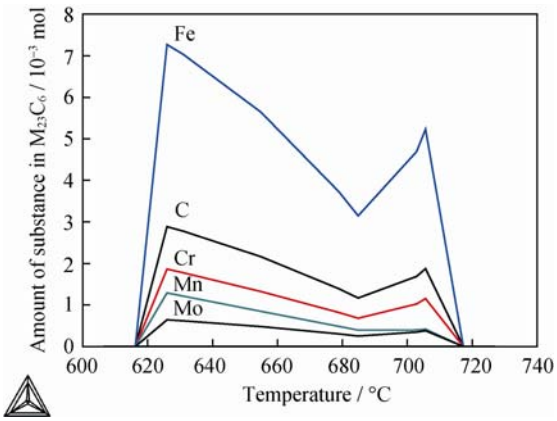

Fig. 5. Chemical elements in $M_{23}C_6$ calculated by Thermo-Calc at 1000 K and 101325 Pa with system size of 1 mol.

Fig. 6 shows the amount of Mo in all phases at different temperatures. The amount of Mo will be various in A (austenite), F (ferrite), $M_{23}C_6$, cementite, and M_7C_3 with decreasing temperature.

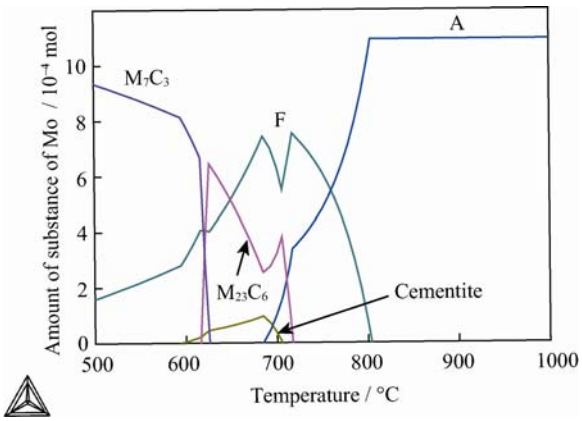

Fig. 6. Amount of Mo in all phases at different temperatures

calculated at 1000 K and 101325 Pa with the system size of 1 mol.

The atom fraction of Mo at grain boundaries was analyzed by electron probe microanalysis (EPMA) on the samples fractured in the hot ductility experiment at 1200°C (Fig. 7). The fracture profile was polished and etched with 4vol% nital for 5 s to display the grain boundary. However, this will change the amount of alloy elements in and out of the grain. Therefore, the shorter the etch time, the higher the accuracy. It is investigated that Mo will segregate at the grain boundary at 1200°C, and the atom fraction will decrease gradually far away from the grain boundary.

The morphology and composition of precipitates in the Mo-containing as-rolled steel was analyzed using TEM; the finishing and coiling temperatures of the steel are 870 and 650°C, respectively. The shape of precipitates is circle or oval shown in Fig. 8(a). Cu comes from the cuprum net of carbon extraction replicas. The precipitates are composed of C, Cr, Si, Mo, and Mn.

Since the coiling temperature is 650°C, M_7C_3 begins to precipitate at 626°C calculated by Thermo-Calc. Moreover, the amount of Mn is the highest in M_7C_3, which is different from the result of energy spectrum analysis. This means that the precipitation is not M_7C_3. However, the amount of Cr is the highest in carbides from carbon extraction replicas, and the chemical composition of the carbides is similar with $M_{23}C_6$. So, the precipitation in the hot rolled strip is composed of $M_{23}C_6$ and cementite. Since Mo inhibits from pearlite formation [17-19], the precipitations of $M_{23}C_6$ will reduce the quantity of Mo dissolving in austenite and ferrite, which promotes the transformation.

Moreover, molybdenum carbides, such as $M_{23}C_6$ and cementite, will dissolve again when the strip is reheated during intercritical annealing. This will improve the hardenability of austenite and increase the martensite volume fraction of the cold-rolled annealed sheet.

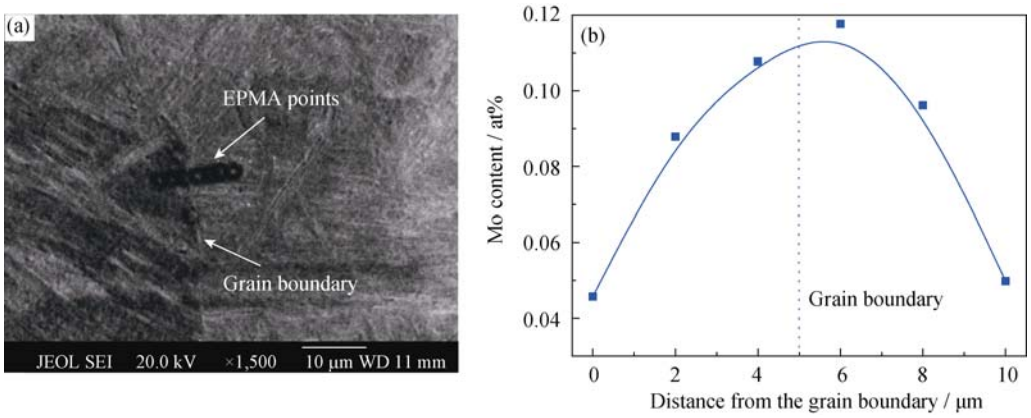

Fig. 7. Segregation of Mo analyzed by EPMA at the grain boundary for the Mo-containing steel at 1200°C: (a) microstructure; (b) atom fraction of Mo at different distances from the grain boundary.

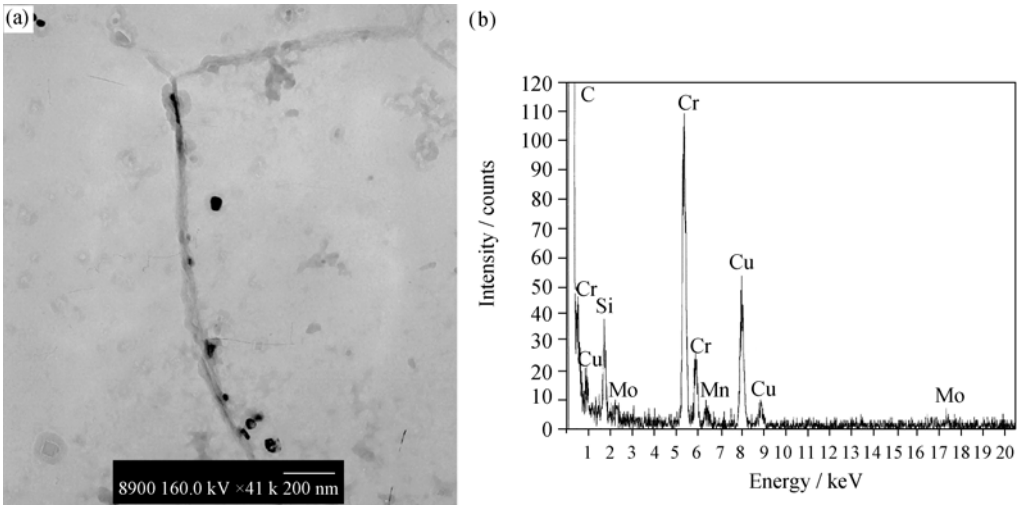

Fig. 8. Morphology (a) and composition (b) of precipitates in the Mo-containing as-rolled steel analyzed by using TEM (finishing temperature: 870°C; coiling temperature: 650°C).

4. Discussion

Due to the segregation of S and P, there is a ductility trough in the Mo-free steel at 800-975°C (Fig. 2). However, this cannot be investigated in the Mo-containing steel. The results are mainly because of the segregation of Mo on grain boundaries, consequently reducing the concentration of P and S, which improves the strength of grain boundaries (Fig. 7).

When the strain rate is 1 s^{-1} in the range of 800-950°C, Mo segregates on moving grain boundaries and consequently delays the nucleation and growth of new grains. Due to the solute drag force and the retardation of precipitation, the migration of the new grains and recrystallization are hindered. However, in the range of 950-1100°C, the effect of Mo segregation on the retardation of recrystallization is not obvious. This can be explained by calculating the enrichment coefficient (α_M) of Mo, Si, Mn, and Cr at the crystal defects.

When the lattice distortion is elastic strain due to solute atoms, the total elastic strain energy is

$$E_E=4G\delta^2V \tag{1}$$

where G is the shear elastic of the matrix, δ the mismatch between two atoms, and V the volume of the solute atom that substitutes the atom of the matrix one.

When the solute atoms segregate on the surfaces of crystals, due to the total relaxation of lattice distortion, the segregation free energy (ΔU) is equal to E_E. While the solute atoms segregate on grain boundaries or phase boundaries, the lattice distortion cannot be relax wholly, namely, $\Delta U \leq E_E$. Moreover, the segregation on grain boundaries and dislocation has the same upper limit of segregation free energy. Therefore, the upper limit of segregation free energy is available by calculation [20].

In consideration of segregation equilibrium thermodynamics, McLean [21] assumes that the crystal defect region is a ruleless ideal solid solution, and there is no interaction between the segregation atoms. Then, a relation is deduced from the solute atoms adsorbed in crystal defects.

$$c_g=\frac{c_0\exp\left(\frac{\Delta U}{kT}\right)}{1-c_0+c_0\exp\left(\frac{\Delta U}{kT}\right)} \tag{2}$$

where c_g is the solute segregation concentration in the crystal defect region, c_0 the solute equilibrium concentration in the matrix, ΔU the segregation free energy, which is the difference value of lattice distortion energy between the perfect crystal and the crystal defect region from solute atoms, k the speed constant, and T the absolute temperature. When $c_0 \ll 1$,

$$c_g=c_0\exp\left(\frac{\Delta U}{kT}\right) \tag{3}$$

The difference value of molar lattice distortion energy is $\Delta G=N_0\cdot\Delta U$ (N_0 is the Avogadro constant). Then,

$$c_g=c_0\exp\left(\frac{\Delta G}{RT}\right) \tag{4}$$

$$\alpha_{\mathrm{M}} = \frac{c_{\mathrm{g}}}{c_0} = \exp\left(\frac{\Delta G}{RT}\right) \quad (5)$$

Furthermore, the α_{M} values of Mo, Si, Mn, and Cr at 500 and 1000°C have been calculated and are listed in Table 2.

Table 2. Enrichment coefficient of solute atoms at the crystal defects

Temperature / °C	Mo	Si	Mn	Cr
1000	2.17	1.18	1.01	1.00
500	8.48	1.59	1.03	1.01

The enrichment ability of Mo, Si, Mn, and Cr at the crystal defects decreases systematically. Moreover, the α_{M} of Mo at 500°C are 4 times higher than that at 1000°C, while the α_{M} of Si, Mn, and Cr increase slightly with decreasing temperature. Therefore, the strength of the Mo-containing steel is higher than the Mo-free one at low temperature due to the segregation of Mo on grain boundaries and crystal defects. In addition, the D-value will increase with decreasing temperature attributing to the difference in α_{M}.

5. Conclusions

(1) Because of the segregation of Mo on grain boundaries, consequently reducing the concentration of P and S, the strength of grain boundaries and hot ductility are improved. Besides, a lower ductility point existing in the Mo-free steels at 850°C is eliminated in the Mo-containing one.

(2) By calculating the α_{M}, the enrichment ability of Mo, Si, Mn, and Cr at crystal defects decreases systematically. Moreover, the α_{M} of Mo at 500°C are 4 times higher than that at 1000°C, while the α_{M} of Si, Mn, and Cr increase slightly with decreasing temperature. Therefore, the strength of the Mo-containing steel is higher than the Mo-free one at low temperature. Moreover, the D-value will increase with decreasing temperature attributing to the difference in α_{M}.

(3) Precipitates in the hot rolled strip are mainly composed of $M_{23}C_6$ and cementite. The precipitates will reduce the amount of Mo dissolving in austenite and ferrite, which promotes pearlite formation. Furthermore, molybdenum carbides will dissolve again when the strip is reheated during intercritical annealing. This will improve the hardenability of austenite and increase the martensite volume fraction of the cold-rolled annealed sheet.

References

[1] H.F. Dong, J. Li, Y. Zhang, *et al*., Numerical simulation on the microstress and microstrain of low Si-Mn-Nb dual-phase steel, *Int. J. Miner. Metall. Mater.*, 17(2010), No.2, p.173.

[2] Y.L. Kang, *Theory and Technology of Processing and Forming for Advanced Automobile Steel Sheets*, Metallurgical Industry Press, Beijing, 2009.

[3] Q. Liu, L.Q. Zhang, L.Z. Wang, *et al*., High temperature mechanical properties of continuously cast blooms for automobile steel, *J. Univ. Sci. Technol. Beijing* (in Chinese), 28(2006), No.2, p.133.

[4] E. Hurtado-Delgado and R.D. Morales, Hot ductility and fracture mechanisms of a C-Mn-Nb-Al steel, *Metall. Mater. Trans. B*, 32(2001), No.5, p.919.

[5] B. Mintz, Influence of composition on the hot ductility of steels and to the problem of transverse cracking, *ISIJ Int.*, 39(1999), No.9, p.833.

[6] S.K. Kim, N.J. Kim, and J.S. Kim, Effect of boron on the hot ductility of Nb-containing steel, *Metall Mater. Trans. A*, 33(2002), No.3, p.701.

[7] H. Wang, W.Y. Liu, and Z.C. Ye, Effect of aluminum amount on the hot ductility of the dual phase steel, *Rare. Met. Mater. Eng.*, 36(2007), Suppl. 3, p.363.

[8] X.H. Wang, B. Chang, J.J. Li, *et al*., Ductility loss and Nb(C, N) precipitation in Nb-containing steel slab in the temperature range from 700 to 1000°C, *Acta Metall. Sin.*, 33(1997), No.5, p.485.

[9] L.H. Chown and L.A. Cornish, Investigation of hot ductility in Al-killed B steels, *Mater. Sci. Eng. A*, 494(2008), No.1-2, p.263.

[10] F. Zarandi and S. Yue, The effect of boron on hot ductility of Nb-microalloyed steels, *ISIJ Int.*, 46(2006), No.4, p.591.

[11] E. López-Chipres, I. Mejía, C. Maldonado, *et al*., Hot ductility behavior of boron microalloyed steels, *Mater. Sci. Eng. A*, 460-461(2007), p.464.

[12] F. Zarandi and S. Yue, Improvement and hot ductility in the Nb-microalloyed steel by high temperature deformation, *ISIJ Int.*, 45(2005), No.5, p.686.

[13] Z. Mohamed, Hot ductility behavior of vanadium containing steels, *Mater. Sci. Eng. A*, 326(2002), p.255.

[14] Y. Saito, T. Enami, and T. Tanaka, Mathematical model of hot deformation resistance with reference to microstructural changes during rolling in plate mill, *Trans. Iron Steel Inst. Jpn.*, 25(1985), p.1146.

[15] M. Dzubinsky, F. Kovac, and A. Petercakova, New form of equation for deformation resistance prediction under hot rolling industrial conditions, *Scripta Mater.*, 47(2002), p.119.

[16] S. Kuang, Y.L. Kang, Q.H. Han, *et al*., Microstructure and properties of cold rolled ultra high strength dual phase steel, [in] *International Symposium on Automobile Steel Proceedings*, Dalian, 2009, p.187.

[17] F.R. Xiao, B. Liao, D.L. Ren, *et al*., Acicular ferritic microstructure of a low-carbon Mn-Mo-Nb microalloyed pipeline steel, *Mater. Charact.*, 54(2005), No.4-5, p.305.

[18] D. Shanmugasundarama and R. Chandramouli, Tensile and

impact behaviour of sinter-forged Cr, Ni and Mo alloyed powder metallurgy steels, *Mater. Des.*, 30(2009), No.9, p.3444.

[19] Y.T. Zhao, S.W. Yang, C.J. Shang, *et al.*, The mechanical properties and corrosion behaviors of ultra-low carbon microalloying steel, *Mater. Sci. Eng. A*, 454-455(2007), p.695.

[20] Q.L. Yong, *Secondary Phases in Steels*, Metallurgical Industry Press, Beijing, 2006.

[21] D. McLean, *Grain Boundaries in Metals*, The Oxford University Press, London, 1957.